Multilevel MATE for Efficient Simultaneous Solution of Control Systems and Nonlinearities in the OVNI Simulator

Mažana Armstrong, *Member, IEEE*, José R. Martí, *Fellow, IEEE*, Luis R. Linares, *Member, IEEE*, and Prabha Kundur, *Fellow, IEEE*

***Abstract*—This paper presents the solution approach for simulation of control systems and nonlinearities used in UBC's Object Virtual Network Integrator (OVNI) power system simulator. OVNI is aimed at simulation of full-size power system networks in real time using integrated software/hardware solutions. The software solution is based on the Multiarea Thévénin Equivalent (MATE) network partitioning framework. Multilevel MATE expands the concept of MATE to a subsystem level, allowing for the efficient inclusion of controllers' equations and nonlinearities.**

***Index Terms*—Controllers, diakoptics, EMTP solution, Multilevel Multiarea Thévénin Equivalent (MATE), nonlinear elements.**

I. Introduction

THE CONCEPT of diakoptics (from the Greek "dia" for "very" and "kopto" for "tearing") was first introduced by Kron in the 1950s [1]. Kron's diakoptics was aimed at the solution of large power system networks with increased computational speeds. The concept exploits the network's sparsity by splitting it into dense subsystems connected by a few links. In [2], Happ recognizes a possibility of multicomputer hardware configurations for application of diakoptics. He proposes the concept of a "cluster of computers" with each computer in the cluster solving a separate part of the whole network.

Sparsity techniques introduced in [3] redirected attention away from diakoptics for the study of large and complex power systems. Only in recent years in the context of real-time simulation [8], and particularly in the case of multicomputer solutions [11], the advantages of diakoptics over sparsity have become strongly manifested.

While both diakoptics and sparsity take advantage of the very sparse nature of the admittance matrix of power networks, diakoptics maintains the identity of the subsystems, a task that is very difficult to achieve in solutions based on matrix reduction with sparsity techniques. Maintaining the individuality of the subsystems permits, for example, pre-calculation of the inverse subsystem matrices for those subsystems that topology does not change, while only some of the subsystems require recalculation. This aspect alone gives diakoptics a considerable advantage over sparsity techniques, and it is a crucial factor in achieving real-time simulation speeds with the Object Virtual Network Integrator (OVNI) simulator.

UBC's OVNI real-time simulator is built around the Multiarea Thévénin Equivalent (MATE) concept [12], which extends the main ideas of diakoptics by recognizing that the subsystems split by the branch links can be represented by Thévénin equivalents. Multilevel MATE further extends the concept of MATE and provides computationally efficient solution framework for controllers and nonlinear elements on a subsystem level.

Manuscript received January 10, 2006; revised March 24, 2006. This work was supported in part by PowertechLabs Inc., Surrey, BC, Canada. Paper no. TPWRS-00006-2006.

M. Armstrong, J. R. Martí, and L. R. Linares are with the Department of Electrical and Computer Engineering, University of British Columbia, Vancouver, BC V3J 1C2, Canada (e-mail: mazanal@ece.ubc.ca).

P. Kundur is with Powertech Labs Inc., Surrey, BC V3W 7R7, Canada.

Digital Object Identifier 10.1109/TPWRS.2006.879254

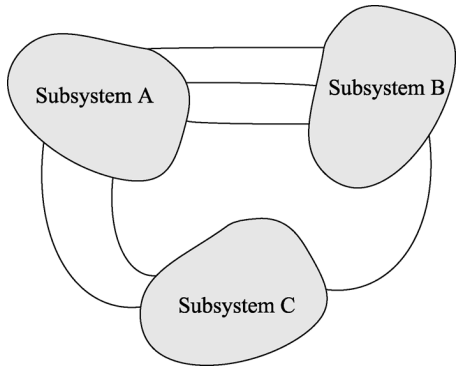

Fig. 1. Example system to demonstrate the MATE concept.

II. Concept of MATE

A. MATE System Partitioning

The original motivation for system partitioning in OVNI was aimed at achieving real-time simulation speed when solving large electric power networks. Additionally, exploiting latency [15] in interfacing "slower" and "faster" subsystems with different simulation steps also contributes to better distribution of computing resources. Another advantage of MATE's system partitioning, as noted earlier, is the separation of subsystems of constant nature and those of changing nature.

To demonstrate the MATE concept, let us consider the system in Fig. 1. Any system can be partitioned into subsystems by the introduction of links (branch equations). For example, the system depicted in Fig. 1 is partitioned into three subsystems

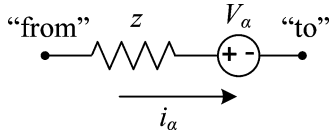

Fig. 2. General description of a link.

A, B, and C, by introducing six links. The hybrid system of modified nodal equations has the following form:

$$\begin{bmatrix} A & 0 & 0 & p \\ 0 & B & 0 & q \\ 0 & 0 & C & r \\ p^t & q^t & r^t & -z \end{bmatrix} \begin{bmatrix} v_A \\ v_B \\ v_C \\ i_\alpha \end{bmatrix} = \begin{bmatrix} h_A \\ h_B \\ h_C \\ -V_\alpha \end{bmatrix} \tag{1}$$

where

— $[A]$, $[B]$, and $[C]$ are subsystems' admittance matrices;
— $[p]$, $[q]$, and $[r]$ are subsystems' current injection (or connectivity) arrays;
— $[z]$ is a matrix of links' Thévénin impedances;
— $[h_A]$, $[h_B]$, and $[h_C]$ are vectors of subsystems' accumulated currents;
— $[V_\alpha]$ is a vector of links' Thévénin voltages;
— $[v_A]$, $[v_B]$, and $[v_C]$ are subsystems' nodal voltages;
— $[i_\alpha]$ is a vector of links' currents.

Connectivity arrays for six links connecting the subsystems are constructed according to [12]. A particular link current is assigned a direction of flow where the "from" node is assigned a "1" in the connectivity array of the "from" subsystem, and the "to" node is assigned a "−1" in the connectivity array of the "to" subsystem. Any component (or branch) in the system can become a link described by its Thévénin impedance (z) and its Thévénin voltage (V_α). The most general representation of a link is depicted in Fig. 2.

Partitioned matrices are manipulated to obtain the subsystems' Thévénin equivalents as seen from the linking nodes. The result of the manipulation is the MATE system of equations of the following form:

$$\begin{bmatrix} 1 & 0 & 0 & a \\ 0 & 1 & 0 & b \\ 0 & 0 & 1 & c \\ 0 & 0 & 0 & z_a \end{bmatrix} \begin{bmatrix} v_A \\ v_B \\ v_C \\ i_a \end{bmatrix} = \begin{bmatrix} e_A \\ e_B \\ e_C \\ e_a \end{bmatrix} \tag{2}$$

where

$$\begin{aligned} a &= A^{-1}p \qquad e_A = A^{-1}h_A \\ b &= B^{-1}q \qquad e_B = B^{-1}h_B \\ c &= C^{-1}\mathrm{r} \qquad e_C = C^{-1}h_C \\ z_\alpha &= p^t a + q^t b + r^t c + z \\ e_\alpha &= p^t e_A + q^t e_B + r^t e_C + V_\alpha. \end{aligned}$$

Note that the individuality of each subsystem is preserved in (2). Vector $[e_A]$ and array $[a]$ represent, respectively, the Thévénin equivalent voltage vector and the Thévénin impedance array of subsystem A as seen from the linking nodes.

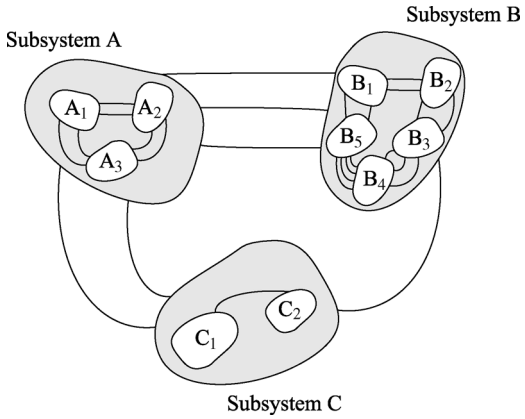

Fig. 3. Example system to demonstrate the "multilevel MATE" concept.

Note that the solution for link currents is now independent from the solution for nodal subsystems' voltages.

The interaction of the three subsystems is solved on the links level and returned to each subsystem in a form of injected currents at linking nodes. The subsystems' nodal equations are then solved independently from each other at the subsystems' level.

B. Multilevel MATE

Multilevel MATE expands the concept of MATE by allowing subsystems to be further partitioned into sub-subsystems, sub-subsystems further partitioned into sub-sub-subsystems, and so forth. A subsystem, for example, can be partitioned into constant and changing structure sub-subsystems, which further contributes to speed up the simulation. As discussed in this paper, multilevel MATE also allows for a very convenient implementation of nonlinearities, including controllers, switches, etc.

The concept of multilevel MATE can be demonstrated on the same system as Fig. 1. This time, the system is further divided into ten sub-subsystems with a total of six links and twenty sublinks, as shown in Fig. 3. The complete system of equations for the depicted system is shown in (3). Matrices $[A]$, $[B]$, and $[C]$ represent the conductance matrices of the corresponding subsystems, while $[p_A]$, $[q_B]$, and $[r_C]$ are the connectivity arrays of the sub-subsystems $(A_1, A_2, \ldots B_1, B_2, \ldots C_1, C_2)$ within the corresponding subsystems

$$\begin{bmatrix} \begin{bmatrix} A & p_A \\ p_A^t & -z_A \end{bmatrix} & 0 & 0 & \begin{bmatrix} p \\ 0 \end{bmatrix} \\ 0 & \begin{bmatrix} B & q_B \\ q_B^t & -z_B \end{bmatrix} & 0 & \begin{bmatrix} q \\ 0 \end{bmatrix} \\ 0 & 0 & \begin{bmatrix} C & r_C \\ r_C^t & -z_C \end{bmatrix} & \begin{bmatrix} r \\ 0 \end{bmatrix} \\ [p^t \quad 0] & [q^t \quad 0] & [r^t \quad 0] & -z \end{bmatrix} \times$$

$$\begin{bmatrix} \begin{bmatrix} v_A \\ i_{A\_sublink} \end{bmatrix} \\ \begin{bmatrix} v_B \\ i_{B\_sublink} \end{bmatrix} \\ \begin{bmatrix} v_C \\ i_{C\_sublink} \end{bmatrix} \\ i_\alpha \end{bmatrix} = \begin{bmatrix} \begin{bmatrix} h_A \\ -V_{A\_sublink} \end{bmatrix} \\ \begin{bmatrix} h_B \\ -V_{B\_sublink} \end{bmatrix} \\ \begin{bmatrix} h_C \\ -V_{c\_sublink} \end{bmatrix} \\ -V_\alpha \end{bmatrix} \tag{3}$$

where

$$[A]=\begin{bmatrix} A_1 & 0 & 0 \\ 0 & A_2 & 0 \\ 0 & 0 & A_3 \end{bmatrix}\quad [B]=\begin{bmatrix} B_1 & 0 & 0 & 0 & 0 \\ 0 & B_2 & 0 & 0 & 0 \\ 0 & 0 & B_3 & 0 & 0 \\ 0 & 0 & 0 & B_4 & 0 \\ 0 & 0 & 0 & 0 & B_5 \end{bmatrix}$$

$$[C]=\begin{bmatrix} C_1 & 0 \\ 0 & C_2 \end{bmatrix}.$$

Matrices $[z_A]$, $[z_B]$, and $[z_C]$ correspond to sublink's Thévénin impedances, and vectors $[V_{A\_sublink}]$, $[V_{B\_sublink}]$, and $[V_{C\_sublink}]$ correspond to sublink's Thévénin voltages.

First, the MATE concept is applied to each subsystem, and the system of (4) is obtained, as shown at the bottom of the page.

Observe that the sublink currents for subsystems A, B, and C, respectively, are

$$\begin{aligned} &\left(p_A^t A^{-1} p_A + z_A\right)\cdot i_{A\_sublink} + p_A^t A^{-1} p \cdot i_\alpha \\ &\quad = p_A^t A^{-1} h_A + V_{A\_sublink} \\ &\left(q_B^t B^{-1} q_B + z_B\right)\cdot i_{B\_sublink} + q_B^t B^{-1} q \cdot i_\alpha \\ &\quad = q_B^t B^{-1} h_B + V_{B\_sublink} \\ &\left(r_C^t C^{-1} r_C + z_C\right)\cdot i_{C\_sublink} + r_C^t C^{-1} r \cdot i_\alpha \\ &\quad = r_C^t C^{-1} h_C + V_{c\_sublink}. \end{aligned} \tag{5}$$

Before applying the MATE concept to the entire system, we note that the sublink currents at the subsystem level in (3) *do not need to be known* at the system level. The computational efficiency of the MATE solution is best maintained if the sublink branch currents are "somehow" made invisible to the top level of the system's partitioning.

Going back to (3), we can remove the equations for the sublink currents from the system of (4), and we can transfer these currents to the right-hand side, as shown in

$$\begin{bmatrix} A & 0 & 0 & p \\ 0 & B & 0 & q \\ 0 & 0 & C & r \\ p^t & q^t & r^t & -z \end{bmatrix} \times \begin{bmatrix} v_A \\ v_B \\ v_C \\ i_\alpha \end{bmatrix} = \begin{bmatrix} h_A - p_A \cdot i_{A\_sublink} \\ h_B - q_B \cdot i_{B\_sublink} \\ h_C - r_C \cdot i_{C\_sublink} \\ -V_\alpha \end{bmatrix}. \tag{6}$$

Equations (5) and (6) fully describe the system. Equation (6) resembles closely the system of original equations for the single-level MATE system partitioning (1). Now MATE is applied to (6) to obtain the following equations:

$$\begin{bmatrix} 1 & 0 & 0 & a \\ 0 & 1 & 0 & b \\ 0 & 0 & 1 & c \\ 0 & 0 & 0 & z_\alpha \end{bmatrix} \times \begin{bmatrix} v_A \\ v_B \\ v_C \\ i_\alpha \end{bmatrix} = \begin{bmatrix} e_A - e_{A\_sublink} \\ e_B - e_{B\_sublink} \\ e_C - e_{C\_sublink} \\ e_\alpha - e_{\alpha\_sublink} \end{bmatrix} \tag{7}$$

where

$$\begin{aligned} e_{A\_sublink} &= A^{-1} p_A \cdot i_{A\_sublink} \\ e_{B\_sublink} &= B^{-1} q_B \cdot i_{B\_sublink} \\ e_{C\_sublink} &= C^{-1} r_C \cdot i_{C\_sublink} \\ e_{\alpha\_sublink} &= p^t e_{A\_sublink} + q^t e_{B\_sublink} + r^t e_{C\_sublink}. \end{aligned} \tag{8}$$

Vectors $[e_{A\_sublink}]$, $[e_{B\_sublink}]$, and $[e_{C\_sublink}]$ represent the contributions of the sublink currents to the Thévénin equivalent voltages of each subsystem, as seen from the linking nodes. By substituting (5) into (8), we can eliminate the sublink currents from the overall system of equations and obtain modified Thévénin impedances and voltages. For subsystem A, for example, $[a]$ and $[e_A]$ represent a Thévénin equivalent, as seen from the linking nodes, as if the sublinks were not present in the system. The modified Thévénin equivalent (MTE) that includes the sublinks' contributions is represented by $[a_{MTE}]$ and $[e_{A\_MTE}]$.

The system of equations for the MTEs is

$$\begin{bmatrix} 1 & 0 & 0 & a_{MTE} \\ 0 & 1 & 0 & b_{MTE} \\ 0 & 0 & 1 & c_{MTE} \\ 0 & 0 & 0 & z_{\alpha\_MTE} \end{bmatrix} \times \begin{bmatrix} v_A \\ v_B \\ v_C \\ i_\alpha \end{bmatrix} = \begin{bmatrix} e_{A\_MTE} \\ e_{B\_MTE} \\ e_{C\_MTE} \\ e_{\alpha\_MTE} \end{bmatrix} \tag{9}$$

where

$$\begin{aligned} a_{MTE} &= a - \Delta a & e_{A\_MTE} &= e_A - \Delta e_A \\ b_{MTE} &= b - \Delta b & e_{B\_MTE} &= e_B - \Delta e_B \\ c_{MTE} &= c - \Delta c & e_{C\_MTE} &= e_C - \Delta e_C \\ z_{\alpha\_MTE} &= p^t a_{MTE} + q^t b_{MTE} + r^t c_{MTE} + z \\ e_{A\_MTE} &= p^t e_{A\_MTE} + q^t e_{B\_MTE} + r^t e_{C\_MTE} + V_\alpha \end{aligned} \tag{10}$$

$$\begin{bmatrix} \begin{bmatrix} 1 & A^{-1}p_A \\ 0 & p_A^t A^{-1} p_A + z_A \end{bmatrix} & 0 & 0 & \begin{bmatrix} A^{-1}p \\ p_A^t A^{-1} p \end{bmatrix} \\ 0 & \begin{bmatrix} 1 & B^{-1}q_B \\ 0 & q_B^t B^{-1} q_B + z_B \end{bmatrix} & 0 & \begin{bmatrix} B^{-1}q \\ q_B^t B^{-1} q \end{bmatrix} \\ 0 & 0 & \begin{bmatrix} 1 & C^{-1}r_C \\ 0 & r_C^t C^{-1} r_C + z_C \end{bmatrix} & \begin{bmatrix} C^{-1}r \\ r_C^t C^{-1} r \end{bmatrix} \\ [p^t \quad 0] & [q^t \quad 0] & [r^t \quad 0] & -z \end{bmatrix} \times$$

$$\begin{bmatrix} \begin{bmatrix} v_A \\ i_{A\_sublink} \end{bmatrix} \\ \begin{bmatrix} v_B \\ i_{B\_sublink} \end{bmatrix} \\ \begin{bmatrix} v_C \\ i_{C\_sublink} \end{bmatrix} \\ i_\alpha \end{bmatrix} = \begin{bmatrix} \begin{bmatrix} A^{-1}h_A \\ p_A^t A^{-1} h_A + V_{A\_sublink} \end{bmatrix} \\ \begin{bmatrix} B^{-1}h_B \\ q_B^t B^{-1} h_B + V_{B\_sublink} \end{bmatrix} \\ \begin{bmatrix} C^{-1}h_C \\ r_C^t C^{-1} h_C + V_{c\_sublink} \end{bmatrix} \\ -V_\alpha \end{bmatrix} \tag{4}$$

and

$$\Delta a = A^{-1}p_A\left(p_A^t A^{-1}p_A + z_A\right)^{-1}p_A^t \cdot a$$
$$\Delta e_A = A^{-1}p_A\left(p_A^t A^{-1}p_A + z_A\right)^{-1} \times \left(p_A^t \cdot e_A + V_{A\_sublink}\right) \quad (11)$$

for subsystem A, with similar expressions for subsystems B and C.

At every time step, each subsystem will pass its modified Thévénin impedances and voltages (i.e., a_{MTE} and e_{A_MTE} for subsystem A) to the links. The system of links is solved first, and the link currents are returned to their corresponding subsystems to obtain the solution for the subsystem voltages. In the case when subsystem links are introduced for the purpose of subsystem partitioning, the sublink currents do not need to be solved. However, if some of the sublinks are nonlinear elements, and it is important to monitor their currents (as, for example, in the case of switches), those sublinks need to be solved at every time step.

Multilevel MATE can be applied to the simulation of switches, ULTC transformers, controllers, nonlinearities, etc. The nonlinearities can affect either the coefficients of the system equations (e.g., machine saturation) or state variables (e.g., nonlinear controllers).

C. Multilevel versus Single-Level MATE

1) Partitioning: It is well established that a partitioned network solved on a cluster of computers is simulated much faster than a non-partitioned one on a single computer [14]. The first level of MATE partitioning is aimed at attaining an optimum computational load distribution among the cluster processors [18].

In the context of the OVNI simulator, the number of link connections between the subsystems is a limiting factor in achieving real-time simulation [17]. High partitioning of the network leads to a faster computation time for subsystems; however, large number of links has the opposite effect on the simulation speed. Multilevel MATE partitioning recognizes the fact that the partitioning (and its corresponding links) that is conceptually necessary to separate parts of a system due to their different nature (i.e., different simulation step requirement, constant versus changing nature) may not in general correspond to the optimal partitioning for the purpose of real-time simulation. Therefore, the second level of MATE partitioning tailored to the subsystem's nature is introduced.

Multilevel MATE introduces a new type of links at the subsystem level that are referred to as *sublinks*. Sublinks can be divided into two categories, partitioning sublinks that are introduced for the purpose of *partitioning* a subsystem, and *functional* sublinks that come from modeling requirements of certain power system components.

Partitioning sublinks are introduced to increase the efficiency of computation by, for example, dividing a subsystem into sub-subsystems of constant and changing nature. A good example of a power system component with changing nature that needs to be updated at every simulation time step is a phase-domain induction or synchronous machine model [9]. Multilevel partitioning also allows for the use of latency [15]. For example, a power electronics device model that requires high frequency switching and therefore very small time step, μs, can be interfaced through sublinks to the rest of the subsystem that can be accurately simulated at a slower rate (ms).

TABLE I
PARTITIONING OF SUBSYSTEM

Subsystem	Number of Sub-subsystems	Number of Sublinks
A	3	6
B	5	13
C	2	1

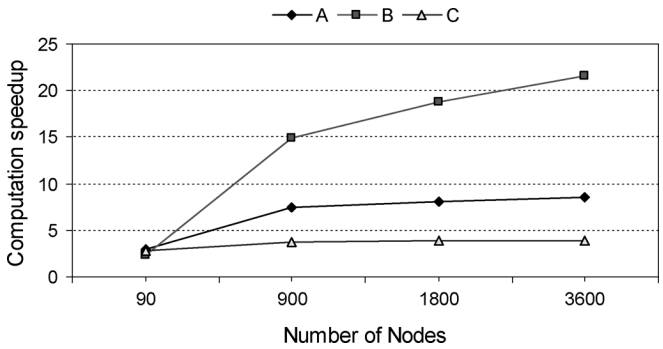

Fig. 4. Multilevel MATE versus single-level MATE computation speedup.

Functional sublinks are branch equations introduced by the modeling requirements of power system components. For example, a controller or a switch will introduce branch equations. Examples are given in the following section. Other power system components that can introduce branch equations are synchronous and induction machines and transformers.

2) Comparison of Computational Efficiency: The benefits of second-level partitioning will be briefly demonstrated on the example of Figs. 1 and 3. Fig. 1 shows a system separated into three subsystems and six links based, for example, on some optimum partitioning algorithm for real-time simulation [18]. It is assumed that each subsystem (A, B, and C) is solved on a separate PC cluster processor [14] and that the links' system of six links communicates with the subsystems at a predefined rate. In Fig. 3, each subsystem is partitioned into sub-subsystems. Because the links' system is unchanged, the simulation speed difference between the single-level and multilevel approach will occur inside the subsystems.

The first assumption made is that subsystems A, B, and C have no functional sublinks. The sublinks that are introduced are only for partitioning purposes. The second assumption is that all the subsystems are of changing nature, and their admittance matrices need to be updated at every time step. This situation is the most computationally demanding scenario.

The comparison is made for the three subsystems with the assumption of the same number of nodes (90, 900, 1800, or 3600) and a different number of partitions and links. According to Fig. 3, Table I is derived.

The computation efficiency of the single-level and multilevel approach is compared in floating point operations (flops) and shown in Fig. 4.

Multilevel MATE reduces the number of computations over 20 times in case of the largest number of nodes for partitioning

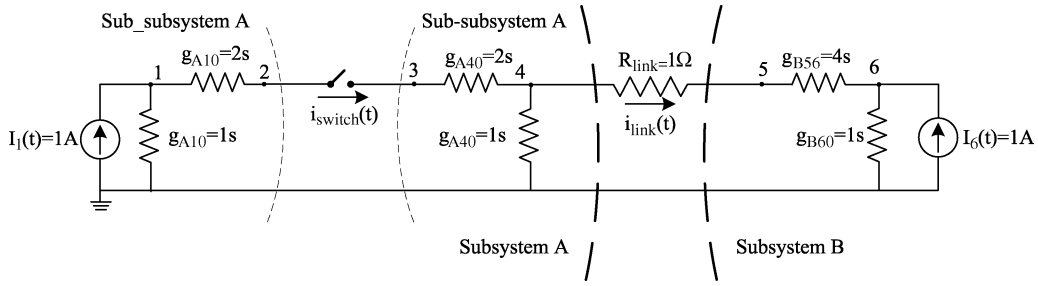

Fig. 5. Example system to demonstrate ideal switching using multilevel MATE concept.

of subsystem B. If some of the subsystems' matrices were constant by nature, their inverses would be precalculated prior to the simulation run time, and the multilevel MATE partitioning would show an even greater increase in calculation speed. In general, for subsystems comprised of changing and constant nature elements and for subsystems that are sparse, the application of the multilevel MATE concept will always lead to a significant computation speedup over the single-level MATE concept.

If conventional sparsity techniques were applied for subsystems with changing topology, each topological change (e.g., switching) within a particular region of the subsystem would require retriangularization of the entire subsystem matrix. With the multilevel MATE concept, the change of topology is confined to the sublinks equations; therefore, the subsystem's matrix need not be recalculated when the change of topology takes place. This allowed us to achieve real-time simulation speed in cases of four-bridge HVDC converters, as discussed in [10].

III. Examples of Multilevel MATE Applications

A. Ideal Switches in OVNI

Multilevel MATE allows switches to be modeled as sublinks within each subsystem. Switching operations involve a change of the subsystem's topology. However, this change can be confined to terms in (11) that are, in effect, modifying the subsystem's Thévénin equivalent, as seen from connecting link nodes.

From (11), it is apparent that the case when a switch in subsystem A is closed simply implies that the corresponding entry of the $[z_A]$ matrix becomes zero ($R_{switch} = 0$). The opening of a switch is reflected in the equations by setting the corresponding entries of Δa and Δe_A to zero, effectively setting the sublink equation to $i_{switch} = 0$.

A simple example system to demonstrate the principles of ideal switching at a subsystem level is depicted in Fig. 5. The system is composed of two subsystems A and B connected through a single link. An ideal switch is placed within subsystem A, and its branch equation is treated as a sublink. The hybrid system of equations is written from (3) in general terms as

$$\left[\begin{array}{cc|c|c|c} A_1 & 0 & p_{A1} & 0 & p_1 \\ 0 & A_2 & p_{A2} & 0 & p_2 \\ \hline p_A^t & & -z_A & 0 & 0 \\ \hline 0 & & 0 & B & q \\ \hline p^t & & 0 & q^t & -z \end{array}\right] \times \left[\begin{array}{c} v_{A1} \\ v_{A2} \\ \hline i_{A\_sublink} \\ \hline v_B \\ \hline i_\alpha \end{array}\right] = \left[\begin{array}{c} h_{A1} \\ h_{A2} \\ \hline -V_{A\_sublink} \\ \hline h_B \\ \hline -V_\alpha \end{array}\right]$$

or for the example system as

$$\left[\begin{array}{cccc|c|cc|c} 3 & -2 & 0 & 0 & 0 & 0 & 0 & 0 \\ -2 & 2 & 0 & 0 & 1 & 0 & 0 & 0 \\ 0 & 0 & 2 & -2 & -1 & 0 & 0 & 0 \\ 0 & 0 & -2 & 3 & 0 & 0 & 0 & 1 \\ \hline 0 & 1 & -1 & 0 & -R_{switch} & 0 & 0 & 0 \\ \hline 0 & 0 & 0 & 0 & 0 & 4 & -4 & -1 \\ 0 & 0 & 0 & 0 & 0 & -4 & 5 & 0 \\ \hline 0 & 0 & 0 & 1 & 0 & -1 & 0 & -1 \end{array}\right] \times \left[\begin{array}{c} v_1 \\ v_2 \\ v_3 \\ v_4 \\ \hline i_{switch} \\ \hline v_5 \\ v_6 \\ \hline i_{link} \end{array}\right] = \left[\begin{array}{c} 1 \\ 0 \\ 0 \\ 0 \\ \hline 0 \\ \hline 0 \\ 1 \\ \hline 0 \end{array}\right].$$

With the switch equation taken out of the system of equations, we apply MATE as in (2) and obtain the subsystems' Thévénin equivalents from

$$a = \begin{bmatrix} A_1^{-1} p_1 \\ A_2^{-1} p_2 \end{bmatrix} = \begin{bmatrix} a_1 \\ a_2 \end{bmatrix} \qquad e_A = \begin{bmatrix} A_1^{-1} h_{A1} \\ A_2^{-1} h_{A2} \end{bmatrix} = \begin{bmatrix} e_{A1} \\ e_{A2} \end{bmatrix}$$
$$b = B^{-1} q \qquad e_B = B^{-1} h_B.$$

The modified Thévénin equivalents are obtained from (10) and (11) as

$$a_{MTE} = a - \Delta a$$
$$e_{A\_MTE} = e_A - \Delta e_A.$$

In general, when an ideal switch is closed, a diagonal element of z_A matrix corresponding to that branch is set to zero ($R_{switch} = 0$). For an ideal switch open, the corresponding column of the subsystem's connectivity array p_A and the row of p_A^t are set to zero, and a diagonal of z_A is set to one ($i_{switch} = 0$).

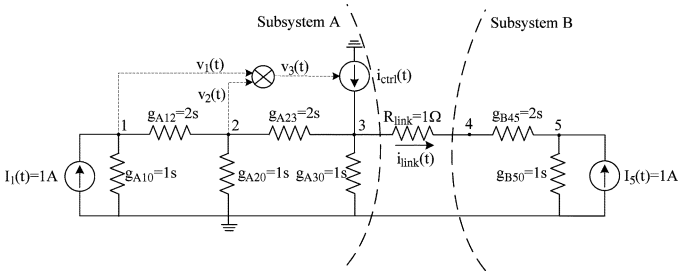

Fig. 6. Example system with a nonlinear controller.

In the example, when the switch is closed, we obtain

$$a_{MTE} = a - \Delta a = \begin{bmatrix} 0 \\ 0 \\ 1 \\ 1 \end{bmatrix} - \begin{bmatrix} -0.3333 \\ -0.5 \\ 0.5 \\ 0.3333 \end{bmatrix} = \begin{bmatrix} 0.3333 \\ 0.5 \\ 0.5 \\ 0.6667 \end{bmatrix}$$

$$e_{A\_MTE} = e_A - \Delta e_A = \begin{bmatrix} 1 \\ 1 \\ 0 \\ 0 \end{bmatrix} - \begin{bmatrix} 0.3333 \\ 0.5 \\ -0.5 \\ -0.3333 \end{bmatrix} = \begin{bmatrix} 0.6667 \\ 0.5 \\ 0.5 \\ 0.3333 \end{bmatrix}$$

and for the switch open

$$a_{MTE} = a - \Delta a = \begin{bmatrix} 0 \\ 0 \\ 1 \\ 1 \end{bmatrix} - \begin{bmatrix} 0 \\ 0 \\ 0 \\ 0 \end{bmatrix} = a$$

$$e_{A\_MTE} = e_A - \Delta e_A = \begin{bmatrix} 1 \\ 1 \\ 0 \\ 0 \end{bmatrix} - \begin{bmatrix} 0 \\ 0 \\ 0 \\ 0 \end{bmatrix} = e_A.$$

The case of an ideal switch implementation with Multilevel MATE can be extended to any element that contributes to a subsystem with branch equations. Such elements include, for example, ideal transformers, controllers, average models of voltage source inverters, and so on.

B. Simulating Nonlinear Controller Equations in OVNI

A traditional approach for the simulation of controllers in power system networks introduces an artificial time-step delay between the network solution and the solution of the control systems. In recent years, different approaches have been proposed to achieve a simultaneous solution of the network and controller equations [7], [13], [16]. Simultaneous solution of nonlinear controllers and the network requires an iterative procedure. The Multilevel MATE approach presented in this paper offers a computationally efficient framework for the iterative solution of nonlinear equations, which is applicable to real-time simulations.

The system in Fig. 6 will be examined to demonstrate the basic principles of solving nonlinear controller equations simultaneously with the network solution. Multiplication of two state variables, for example, makes a control scheme in this example nonlinear. The system in question is partitioned into two subsystems, A and B, with subsystem A containing a nonlinear control equation that controls the voltage of node "3." The partitioned system equations can be written in general terms as

$$\left[\begin{array}{c|c|c|c} A & p_{A\_ctrl} & \frac{0}{0} & \frac{p}{0} \\ \hline p^t_{A\_ctrl} & -z_{A\_ctrl} & & \\ \hline 0 \mid 0 & & B & q \\ \hline p^t \mid 0 & & q^t & -z \end{array}\right] \times \left[\begin{array}{c} \frac{v_A}{i_{A\_ctrl}} \\ \hline v_B \\ \hline i_\alpha \end{array}\right] = \left[\begin{array}{c} \frac{h_A}{-V_{A\_ctrl}} \\ \hline h_B \\ \hline -V_\alpha \end{array}\right] \quad (12)$$

where V_{A_ctrl} is a nonlinear controller function.

For the example system

$$\left[\begin{array}{ccc|c|cc|c} 3 & -2 & 0 & 0 & 0 & 0 & 0 \\ -2 & 5 & -2 & 0 & 0 & 0 & 0 \\ 0 & -2 & 3 & -1 & 0 & 0 & 1 \\ \hline 0 & 0 & -1 & 0 & 0 & 0 & 0 \\ \hline 0 & 0 & 0 & 0 & 2 & -2 & -1 \\ 0 & 0 & 0 & 0 & -2 & 3 & 0 \\ \hline 0 & 0 & 1 & 0 & -1 & 0 & -1 \end{array}\right] \times \left[\begin{array}{c} v_1^{(i)}(t) \\ v_2^{(i)}(t) \\ \hline v_3(t) \\ \hline i_{ctrl}^{(i)}(t) \\ \hline v_4(t) \\ \hline v_5(t) \\ \hline i_{link}^{(i)}(t) \end{array}\right] = \left[\begin{array}{c} 1 \\ 0 \\ \hline 0 \\ \hline -v_1^{(i-1)}(t) \cdot v_2^{(i-1)}(t) \\ \hline 0 \\ \hline 1 \\ \hline 0 \end{array}\right]. \quad (13)$$

Note that the branch equation for the controller's current $i_{ctrl}(t)$ in (13) is, indeed, nonlinear. Generally speaking, the controller equations (linear and nonlinear) will affect the structure of $p^t_{A\_ctrl}$, and the array $p^t_{A\_ctrl}$ will no longer be a transpose of the connectivity array $p^t_{A\_ctrl}$ [16].

Following the procedure explained for the multilevel MATE concept, MATE is applied to subsystem A to extract the nonlinear equation in the following general form:

$$\left(p^t_{A\_ctrl} \cdot A^{-1} \cdot p_{A\_ctrl} + z_{A\_ctrl}\right) \cdot i_{A\_ctrl}(t) + p^t_{A\_ctrl} \cdot A^{-1} \cdot p \cdot i_\alpha(t) = p^t_{A\_ctrl} \cdot A^{-1} \cdot h_A + V_{A\_ctrl}. \quad (14)$$

The system of equations is then reduced by moving the unknown controller current to the right-hand side of the system of equations in (12)

$$\left[\begin{array}{c|c|c} A & [0] & p \\ \hline [0] & B & q \\ \hline p^t & q^t & -z \end{array}\right] \cdot \left[\begin{array}{c} \frac{v_A}{v_B} \\ \hline i_\alpha \end{array}\right] = \left[\begin{array}{c} \frac{h_A - p_{A\_ctrl} \cdot i_{A\_ctrl}}{h_B} \\ \hline -v_\alpha \end{array}\right]. \quad (15)$$

In the next step, we apply MATE to (15) to obtain the following MATE system of equations:

$$\left[\begin{array}{c|c|c} [I] & [0] & a \\ \hline [0] & [I] & b \\ \hline [0] & [0] & z_\alpha \end{array}\right] \cdot \left[\begin{array}{c} v_A \\ \hline v_B \\ \hline i_\alpha \end{array}\right] = \left[\begin{array}{c} e_A - \Delta e_{A\_ctrl} \\ \hline e_B \\ \hline e_\alpha - e_{\alpha\_ctrl} \end{array}\right] \tag{16}$$

where

$$\Delta e_{A\_ctrl} = A^{-1} p_{A\_ctrl} \cdot i_{A\_ctrl}$$
$$e_{\alpha\_ctrl} = p^t \Delta e_{A\_ctrl}.$$

At each solution time step, subsystem A assumes the last known value of the controller current i_{A_ctrl} and calculates its contribution to the subsystem's Thévénin equivalent voltage Δe_{A_ctrl}. The modified Thévénin equivalent of subsystem A is then passed to the links to obtain the link current from

$$i_\alpha = z_\alpha^{-1}(e_\alpha - e_{\alpha\_ctrl}). \tag{17}$$

The link current is returned to subsystem A. The nonlinear controller element requests from its subsystem the values of the link currents and voltages needed to recalculate its nonlinear (14). The new value of i_{A_ctrl} is passed back to subsystem A in order to recalculate its modified Thévénin equivalent voltage. The modified Thévénin equivalent voltage of subsystem A is then passed to the links, and a new value of the link current is obtained. Iterations are repeated until the nonlinear element satisfies its solution tolerance and raises a flag for the simulation to proceed to the next time step.

For the example in Fig. 6, (16) becomes

$$\left[\begin{array}{ccc|cc|c} 1 & 0 & 0 & 0 & 0 & 0.19048 \\ 0 & 1 & 0 & 0 & 0 & 0.28571 \\ 0 & 0 & 1 & 0 & 0 & 0.19048 \\ \hline 0 & 0 & 0 & 1 & 0 & -1.5 \\ 0 & 0 & 0 & 0 & 1 & 1 \\ \hline 0 & 0 & 0 & 0 & 0 & 3.0238 \end{array}\right] \cdot \left[\begin{array}{c} v_1^{(i)}(t) \\ v_2^{(i)}(t) \\ \hline v_3(t) \\ v_4(t) \\ v_5(t) \\ \hline i_{link}^{(i)}(t) \end{array}\right]$$
$$= \left[\begin{array}{c} 0.52381 + 0.19048 \cdot i_{ctrl}^{(i-1)}(t) \\ 0.28571 + 0.28571 \cdot i_{ctrl}^{(i-1)}(t) \\ \hline 0.19048 + 0.52381 \cdot i_{ctrl}^{(i-1)}(t) \\ \hline 1 \\ 1 \\ \hline -0.80952 + 0.52381 \cdot i_{ctrl}^{(i-1)}(t) \end{array}\right]$$

where i is the iteration step.

In the first iteration, we assume $i_{ctrl}^{(0)}(t) = 0$ and calculate

$$\text{From (17)}: \quad i_{link}^{(1)}(t) = -0.2677[\text{A}]$$
$$\text{From (16)}: \quad v_{A\_ctrl}^{(1)}(t) = \begin{bmatrix} v_1^{(1)}(t) \\ v_2^{(1)}(t) \end{bmatrix} = \begin{bmatrix} 0.5748 \\ 0.3622 \end{bmatrix} [\text{V}]$$
$$\text{From (14)}: \quad i_{ctrl}^{(1)}(t) = -0.2339[\text{A}].$$

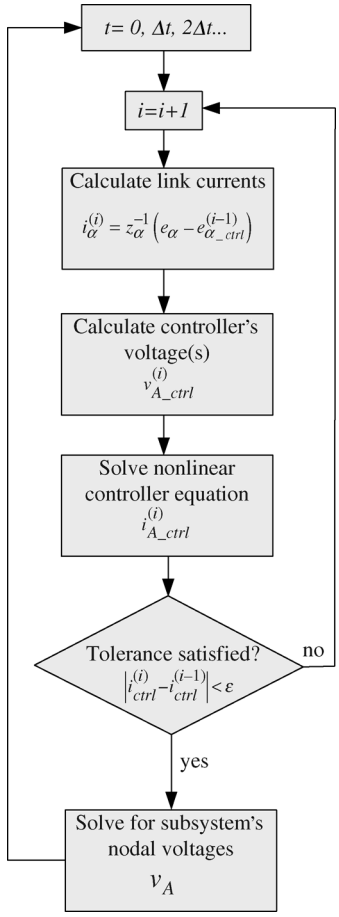

Fig. 7. Flow chart of iteration process for nonlinear controllers.

Iterations are continued until the desired tolerance is achieved. The procedure is depicted as a flow chart in Fig. 7.

The nonlinear controller iterates the solution for its current against the link equations alone. If there were more nonlinear controllers in the system, each one would perform its iterating procedure in the same manner, with the overall solution for nonlinearities being integrated at the links level.

For slow-changing control variables in power system networks (e.g., rms values of system voltages and currents), the algorithm automatically recognizes that the iteration procedure is not needed. In other words, the links solution is based on the present time step of the subsystems' Thévénin equivalents and the previous time step of the nonlinear currents. The values of the present time step nonlinear controller currents are calculated from the nonlinear equations and are used to obtain the present time-step nodal subsystem voltages.

C. Single-Machine Infinite Bus Case Study

The MATE concept was initially developed for UBC's OVNI real-time simulator that is based on the EMTP type of analysis. However, the MATE and the Multilevel MATE approaches are not limited to the EMTP type of analysis. On the contrary, the approaches are applicable to any type of power system analysis

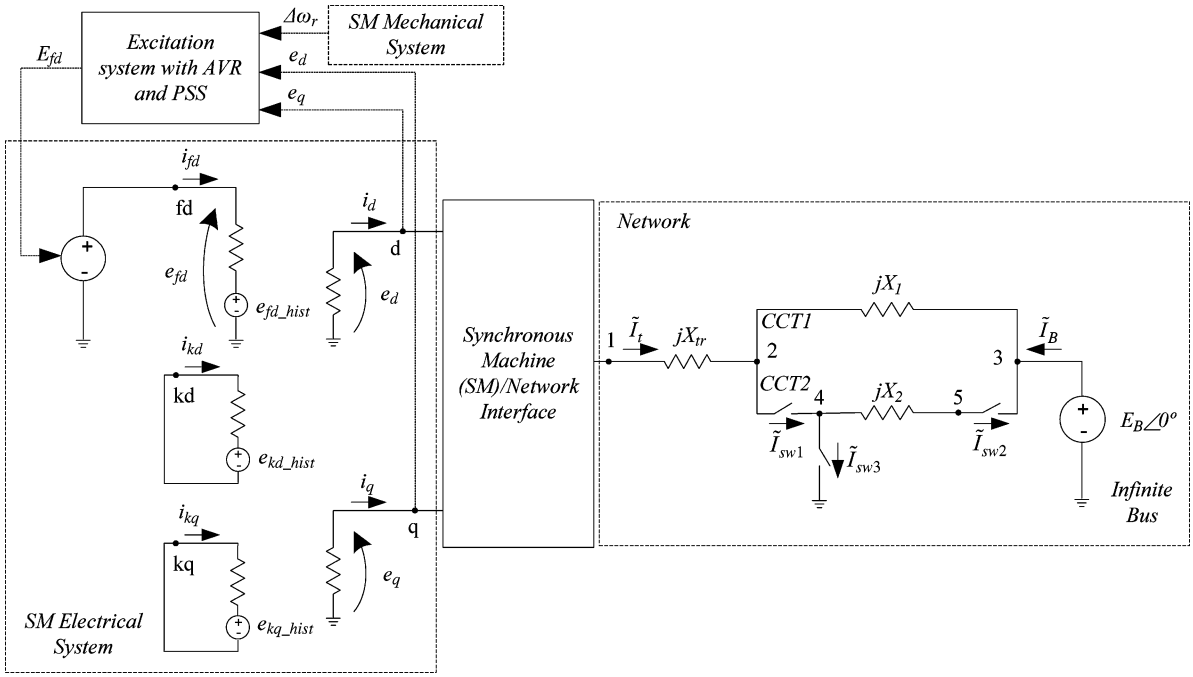

Fig. 8. Single-machine infinite bus system.

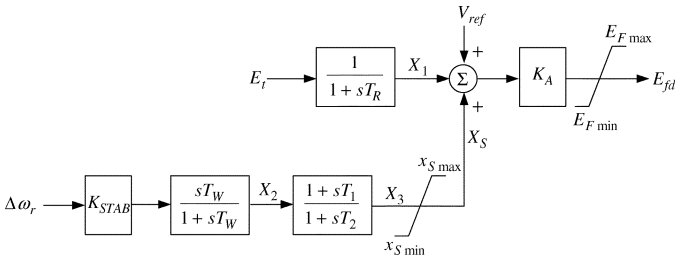

Fig. 9. Tyristor excitation system with AVR and PSS.

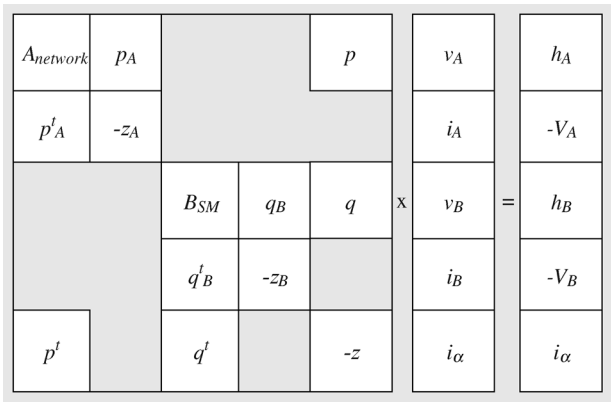

Fig 10. Multilevel MATE partitioning of the single-machine infinite bus system.

or, in more general terms, to any type of electric circuit analysis. The purpose of this case is to demonstrate the applicability of the Multilevel MATE approach to a typical transient stability study.

A single-machine infinite bus power system from [5] is solved using the Multilevel MATE approach. The system consists of an equivalent synchronous generator representing four generating units of a power plant, a step-up transformer, and a double circuit transmission line connecting the generator to a large power system represented by an infinite bus. The synchronous generator is modeled in the dq reference frame, including the rotor dynamics and a bus fed thyristor excitation system with an automatic voltage regulator (AVR) and power system stabilizer (PSS). Network transients as well as stator transients have been neglected, as it is traditionally done in power system transient stability analysis. The electrical discrete time circuit of the example system is shown in Fig. 8.

Differential equations associated with the circuit have been discretized using the implicit trapezoidal integration rule. In general, discretization can be achieved by mapping the Laplace operator s to the z-domain with an integration step Δt

$$s = \frac{2}{\Delta t} \cdot \frac{1 - z^{-1}}{1 + z^{-1}}. \tag{18}$$

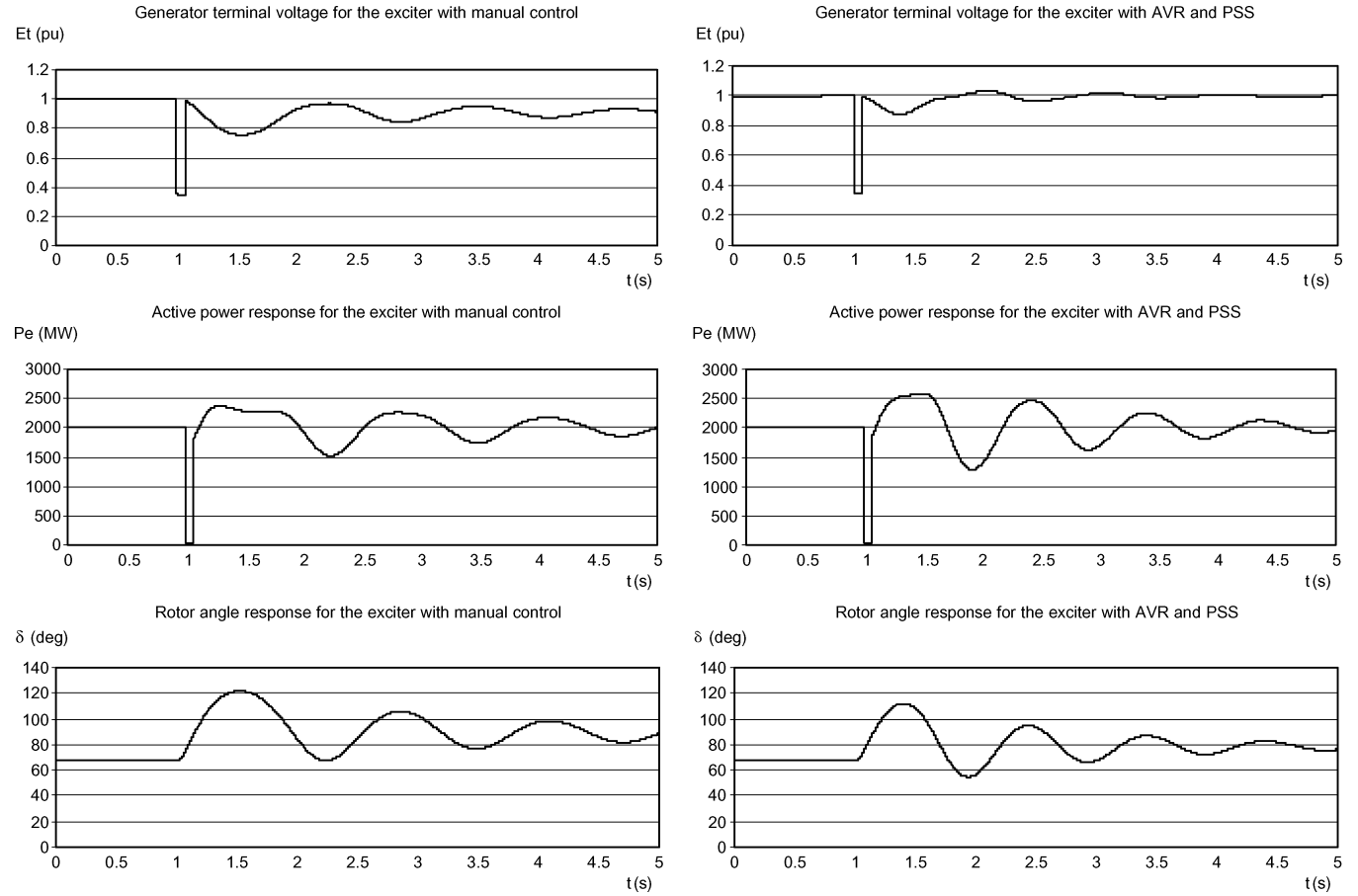

Fig 11. Transient response of the single-machine infinite bus system with fault cleared in 0.07 s.

This mapping can be applied directly to the exciter transfer functions shown in Fig. 9

$$
\begin{aligned}
&-E_t(t)+\left(1+T_R\frac{2}{\Delta t}\right)x_1(t)\\
&\quad=E_t(t-\Delta t)-\left(1-T_R\frac{2}{\Delta t}\right)x_1(t-\Delta t)\\
&\qquad-\left(1+T_1\frac{2}{\Delta t}\right)x_2(t)+\left(1+T_2\frac{2}{\Delta t}\right)x_3(t)\\
&\quad=\left(1-T_1\frac{2}{\Delta t}\right)x_2(t-\Delta t)-\left(1-T_2\frac{2}{\Delta t}\right)x_3(t-\Delta t)\\
&\qquad-K_{STAB}\left(T_W\frac{2}{\Delta t}\right)\Delta\omega_r(t)+\left(1+T_W\frac{2}{\Delta t}\right)x_2(t)\\
&\quad=-K_{STAB}\left(T_W\frac{2}{\Delta t}\right)\Delta\omega_r(t-\Delta t)\\
&\qquad-\left(1-T_W\frac{2}{\Delta t}\right)x_2(t-\Delta t)
\end{aligned}
$$

$$
\begin{cases}
-x_3(t)+x_S(t)=0, & \text{for } x_{S\min}\le x_S\le x_{S\max}\\
x_S(t)=x_{S\max}, & \text{for } x_{S\max}<x_S\\
x_S(t)=x_{S\min}, & \text{for } x_S<x_{S\min}
\end{cases}
$$

$$
\begin{cases}
E_{fd}(t)+K_A\left(x_1(t)-x_S(t)\right)\\
\quad=K_AV_{ref}, & \text{for } E_{F\min}\le E_{fd}\le E_{F\max}\\
E_{fd}=E_{F\max}, & \text{for } E_{F\max}<E_{fd}\\
E_{fd}=E_{F\min}, & \text{for } E_{fd}<E_{F\min}
\end{cases}
$$

where

— E_t is the synchronous machine stator terminal voltage;

— $\Delta\omega_r$ is per unit relative rotor angular velocity;

— $E_{fd}=(L_{adu}/R_{fd})e_{fd}$ is the exciter output voltage.

The Multilevel MATE system partitioning is applied to separate the main components of the system: *the network* and *the synchronous machine* with *the exciter*. The system partitioning structure is shown in Fig. 10, where

— v_A represents the networks branch voltages in dq reference frame;

— i_A represents the networks branch currents, including the equations for ideal switches ($I_{sw1}, I_{sw2}\ldots$ in Fig. 8) in dq reference frame;

— v_B represents synchronous machine stator and rotor voltages and the rotor angle;

— i_B represents synchronous machine stator and rotor currents, relative rotor angular velocity, internal variables of the exciter (X_1, X_2, and X_3 in Fig. 9) and nonlinear equations for electromagnetic torque, terminal voltage magnitude E_t, and the exciter's limited variables (X_s and E_{fd} in Fig. 9);

— i_α represents connecting links for terminal current (I_t) and infinite bus current (I_B) in dq coordinates and the rotor angle link δ.

A transient response of the system variables to a three-phase short circuit applied on Circuit 2 of the transmission line is simulated using the multilevel MATE approach. The results for the system's currents and voltages as well as for the synchronous machine mechanical variables are depicted in Fig. 11. The results agree with the time responses presented in [5].

IV. Conclusion

OVNI is UBC's power system simulator based on the MATE concept for network partitioning. MATE splits the network into subsystems by the introduction of links. By choosing the subsystems to be dense, MATE achieves the advantages of sparsity without sacrificing the identity of the subsystems. Individual subsystems are solved separately, and the overall solution is combined at the level of their Thévénin equivalents.

Multilevel MATE is a new concept that expands the concept of MATE to a subsystem level. Subsystems are further partitioned by the introduction of sublinks. Sublinks can represent, for example, elements at the subsystem level that are better described by their branch equation(s), as opposed to their modeling using nodal equation(s). An example of such an element is an ideal switch or an ideal transformer model. A new approach is presented here that first separates the subsystem's branch equations from the nodal equations and then combines the solution into a MTE at the subsystem level. This approach maintains the size and identity of the subsystems' nodal equations.

The concept of Multilevel MATE is extended in this paper for the simultaneous solution of linear and nonlinear control blocks. A very efficient iteration algorithm can be implemented in the case of nonlinear control blocks (or other nonlinear elements) that takes advantage of the fact that linear parts of the network do not need to be re-triangularized.

References

[1] G. Kron, "Tensorial analysis of integrated transmission systems, part III—the primitive division," *AIEE Trans.*, vol. 71, pt. 3, pp. 814–821, 1952.

[2] H. H. Happ, "Diakoptics—the solution of system problems by tearing," *Proc. IEEE*, vol. 62, no. 7, pp. 930–940, Jul. 1974.

[3] W. F. Tinney and J. W. Walker, "Direct solution of sparse network equations by optimally ordered triangular factorization," *Proc. IEEE*, vol. 55, no. 11, pp. 1801–1809, Nov. 1967.

[4] H. W. Dommel, *EMTP Theory Book*, 2nd ed. Vancouver, BC, Canada: Microtran Power Systems Analysis Corp., 1992–1996, pp. 12-3–12-9.

[5] P. Kundur, *Power System Stability and Control*. New York: McGraw Hill, 1994.

[6] C. W. Ho, A. E. Ruehli, and P. A. Brennan, "The modified nodal approach to network analysis," *IEEE Trans. Circuits Syst.*, vol. CAS-22, pp. 504–509, Jun. 1975.

[7] A. E. A. Araujo, H. W. Dommel, and J. R. Marti, "Simultaneous solution of power and control systems equations," *IEEE Trans. Power Syst.*, vol. 8, no. 4, pp. 1483–1489, Nov. 1993.

[8] J. R. Martí and L. R. Linares, "Real-time EMTP-based transients simulation," *IEEE Trans. Power Syst.*, vol. 9, no. 3, pp. 1309–1317, Aug. 1994.

[9] J. R. Marti and K. W. Louie, "A phase-domain synchronous generator model including saturation effects," *IEEE Trans. Power Syst.*, vol. 12, no. 1, pp. 222–229, Feb. 1997.

[10] S. Acevedo, L. R. Linares, J. R. Martí, and Y. Fujimoto, "Efficient HVDC converter model for real time transients simulation," *IEEE Trans. Power Syst.*, vol. 14, no. 1, pp. 166–171, Feb. 1999.

[11] J. R. Martí, J. A. Hollman, and J. Calvino-Fraga, "Implementation of a real-time distributed network simulator with PC-clusters," in *IEEE Computer Soc. Proc. (PARELEC'2000)* , Trois-Rivières, QC, Canada, Aug. 27–30, 2000.

[12] J. R. Martí, L. R. Linares, J. A. Hollman, and F. M. Moreira, "OVNI: integrated software/hardware solution for real-time simulation of large power systems," in *Proc. 14th Power Systems Computation Conf. (PSCC02)*, Sevilla, Spain, Jun. 24th–28th, 2002.

[13] B. D. Bonatto and H. W. Dommel, "A circuit approach for the computer modelling of control transfer functions," in *Proc. 14th Power Systems Computation Conf. (PSCC02)*, Sevilla, Spain, Jun. 24th–28th, 2002.

[14] J. A. Hollman and J. R. Marti, "Real time network simulation with PC-cluster," *IEEE Trans. Power Syst.*, vol. 18, no. 2, pp. 563–569, May 2003.

[15] F. A. Moreira and J. R. Marti, "Latency techniques for time-domain power system transients simulation," *IEEE Trans. Power Syst.*, vol. 20, no. 1, pp. 246–253, Feb. 2005.

[16] L. Linares, M. Armstrong, and J. R. Martí, "Software implementation of controller representation in the OVNI simulator," in *Proc. 15th Power Systems Computation Conf. (PSCC05)*, Liège, Belgium, Aug. 22th–26th, 2005.

[17] T. De Rybel, J. A. Hollman, and J. R. Marti, "OVNI-NET: a flexible cluster interconnect for the New OVNI real-time simulator," in *Proc. 15th Power Systems Computation Conf. (PSCC05)*, Liège, Belgium, Aug. 22th–26th, 2005.

[18] P. Zhang, J. R. Marti, and H. W. Dommel, "Network partitioning for real-time power system simulation," in *Proc. 6th Int. Conf. Power Systems Transients (IPST'05)*, Montreal, QC, Canada, Jun. 19–23, 2005.

Mazana Armstrong (M'98) received the electrical engineer degree from the University of Zagreb, Zagreb, Croatia, in 1995 and the M.A.S. degree in 2000 from The University of British Columbia, Vancouver, BC, Canada, where she is currently pursuing the Ph.D. degree.

She joined Croatian Power Utility (HEP) Distribution Company ("Elektra") in 1996, where she worked as a Research Engineer in the Department for Planning of Distribution Networks of the city of Zagreb until 1997. She joined Energy Institute "Hrvoje Pozar," Zagreb, in 1997, where she worked as a Research Assistant in the Department for Energy Generation and Transformation until 1999. Her main research interests are development and implementation of new solution techniques for offline and real-time simulations of large power system networks.

Ms. Armstrong is the Chair of the IEEE Vancouver Section Industry Applications Society.

José R. Martí (F'02) received the electrical engineer degree from Central University of Venezuela, Caracas, in 1971, the M.E.E.P.E. degree from Rensselaer Polytechnic Institute, Troy, NY, in 1974, and the Ph.D. degree in electrical engineering from the University of British Columbia, Vancouver, BC, Canada, in 1981.

He is a Professor of electrical and computer engineering at the University of British Columbia. He is known for his contributions to the modeling of fast transients in large power networks, including component models and solution techniques. Particular emphasis in recent years has been on the development of distributed computational solutions for real-time simulation of large systems.

Dr. Martí is a Registered Professional Engineer in the Province of British Columbia, Canada.

Luis R. Linares (M'05) received the electrical engineer degree from Central University in Venezuela, Caracas, in 1981 and the M.A.S. and Ph.D. degrees from the University of British Columbia (UBC), Vancouver, BC, Canada, in 1993 and 2000, respectively.

He has worked in industry full time, and later as a consultant, in projects for companies in Canada, the United States, South America, Europe, and Japan. In 2001, he became a full-time member of the faculty body of the UBC Electrical and Computer Engineering Department and was granted early tenure in 2005. His research interests include real-time simulation of engineering systems, operating systems, and education in engineering. He is currently the coordinator of the Information Technology Minor of the Faculty of Applied Sciences of UBC.

Prabha Kundur (F'85) received the Ph.D. degree in electrical engineering from the University of Toronto, Toronto, ON, Canada, in 1967.

He is President and CEO of Powertech Labs, Surrey, BC, Canada. Prior to joining Powertech in 1993, he worked at Ontario Hydro for 25 years and was involved in the planning and design of power systems. He has served as an Adjunct Professor at the University of British Columbia, Vancouver, BC, Canada, since 1979.

Dr. Kundar is the immediate past-chairman of the IEEE Power System Dynamic Performance Committee. He is also active in CIGRE and is currently the chairman of the CIGRE Study Committee C4. He is the recipient of the 1997 IEEE Nikola Tesla Award, the 1999 CIGRE Technical Committee Award, and the 2005 IEEE PES Charles Concordia Power System Engineering Award. He has been awarded two honorary degrees: Doctor Honoris Causa by the University Politechnica of Bucharest in 2003 and Doctor of Engineering, Honoris Causa by the University of Waterloo in 2004.